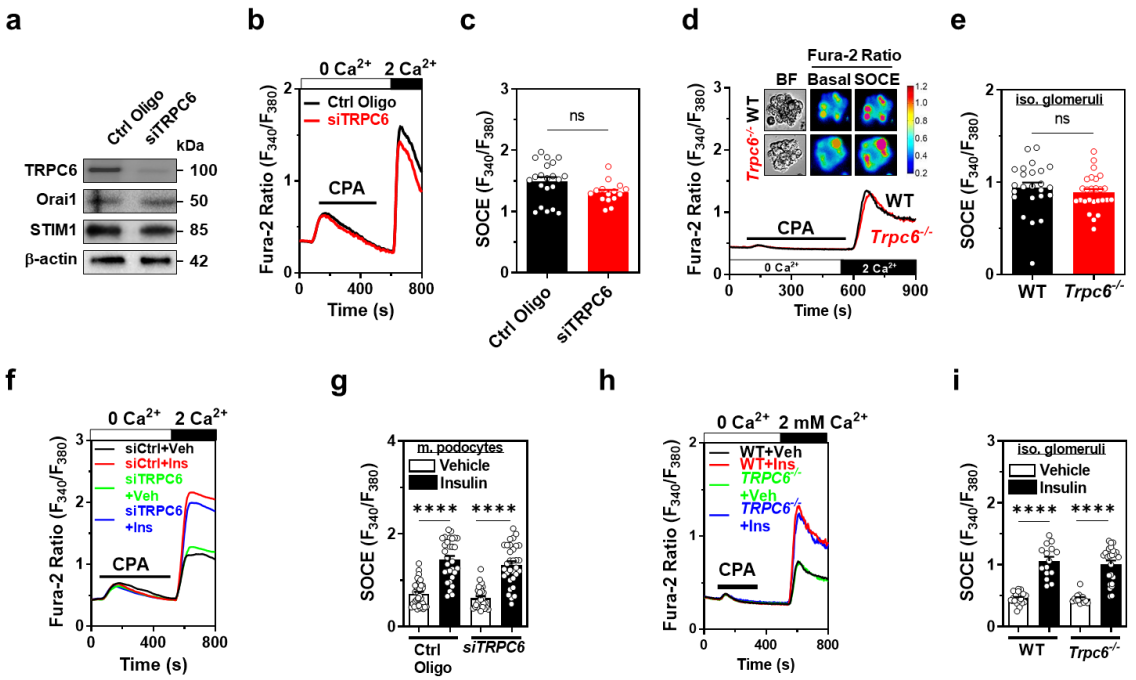


**Supplementary Fig. 1 TRPC6 may not participate in store-operated $Ca^{2+}$ entry (SOCE) in podocyte.**

**a** Effect of TRPC6 siRNA knockdown on the expression of Orai1 and STIM1 in mouse podocytes. Repeated 3 independent experiments. **b** Representative traces of fura-2 ratio representing the effect of TRPC6 silencing on SOCE in podocytes. **c** Summary of the SOCE in panel (**b**). *n* = 21 and 15 cells, respectively. **d** Representative fluorescence images (upper panel) and traces of fura-2 ratio (lower panel) in acutely isolated mouse glomeruli from wild type (WT) and *Trpc6*$^{-/-}$ mice. **e** Summary of the SOCE in panel (**d**). *n* = 24 (WT), and 26 (*Trpc6*$^{-/-}$) glomeruli. **f** Representative SOCE traces showing the effect of TRPC6 knockdown on insulin-stimulated SOCE in cultured mouse podocytes. **g** Summary of the SOCE in panel (**f**). *n* = 37, 30, 28, 32 cells per each group. **h** Representative SOCE traces showing insulin (100 nM, 1 h)-activated SOCE in acutely isolated mouse glomeruli from WT and *Trpc6*$^{-/-}$ mice. **i** Summary of the SOCE in panel (**h**)**.** *n* = 21, 15, 14, and 24 glomeruli each. Data are expressed as mean ± SEM analyzed with unpaired two-tailed Student's *t*-test to Ctrl Oligo and WT (**c** and **e**) and two-way ANOVA followed by Tukey's multiple comparisons test (**g** and **i**). ****$p < 0.0001$, ns., not significant.

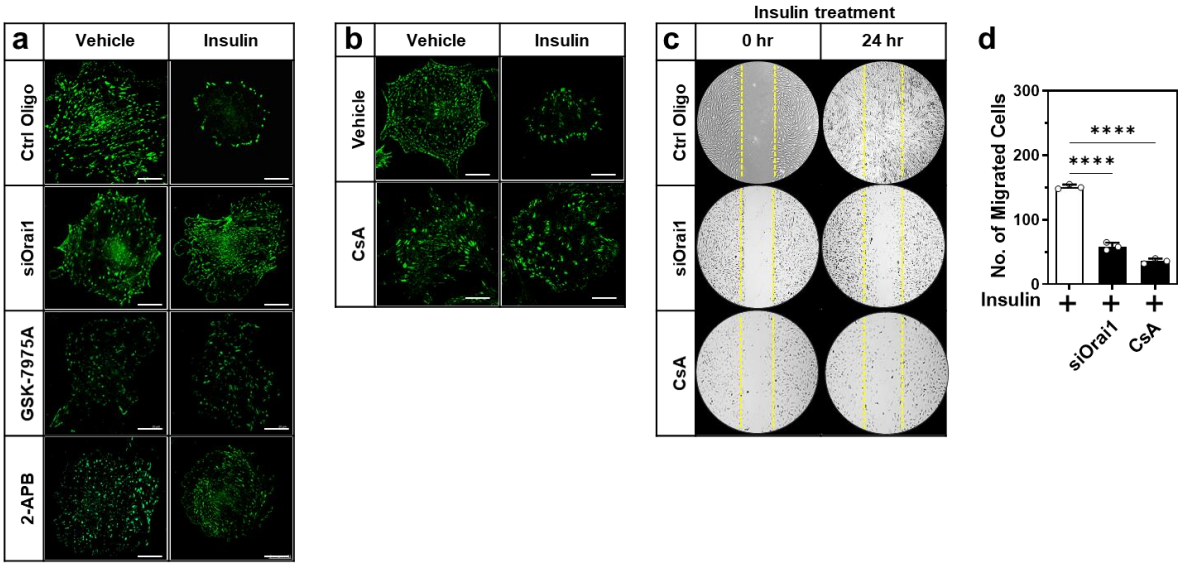


**Supplementary Fig. 2 Insulin stimulation of Orai1 promotes disruption of focal adhesion and cell migration.**

**a** Effect of Orai1 inhibition by siRNA knockdown or its blockers, GSK-7975A (3 μM) or 2-APB (100 μM), on insulin-induced redistribution of paxillin in cultured mouse podocytes. **b** Effect of cyclosporine A (CsA; 10 μM) on insulin-mediated redistribution of paxillin in cultured mouse podocytes. Scale bar = 50 μm., All images were represented similarly from 3 independent experiments and randomly chosen10~12 cells in each dish (**a** and **b**). **c** Scratch assay showing the effect of siRNA Orai1 (siOrai1) and CsA on insulin-stimulated podocyte motility. **d** Cell motility was evaluated by counting the number of migrated cells into the wound area after 24 h. $n$ = 3 independent experiments. Data are expressed as mean ± SEM and analyzed with one-way ANOVA followed by Dunnett's multiple comparisons test (**d**). ****$p < 0.0001$.

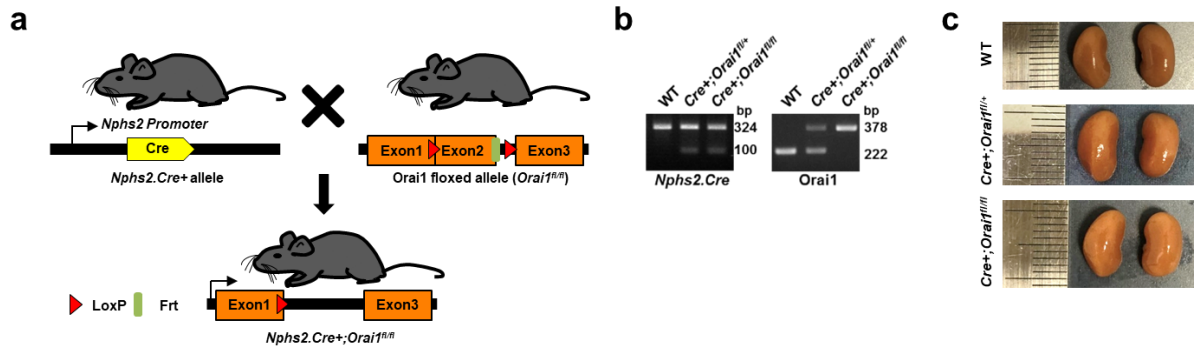


**Supplementary Fig. 3 Construction and macroscopic kidneys of podocyte-specific *Orai1*-deletion mice.**

**a** Schematic representation of the *Nphs2.Cre*+ (upper left) and *Orai1*$^{fl/+}$ (upper right) mice to generate podocyte-specific Orai1 knockout. Exon 2 of the Orai1 gene was targeted[46] in the *Nphs2.Cre*+;*Orai1*$^{fl/fl}$ mice (lower). **b** Germ-line transmission of Cre and flox alleles was validated by genotyping PCR. The 324-base pair (bp) band is the international positive control and the 100 bp band denotes *Nphs2.Cre*+(left). The 378-base pair (bp) band is derived from the floxed allele while the 222-bp band denotes the wild-type (WT) allele (right). **c** No difference in kidney size was observed between podocyte-specific Orai1 knockout and WT mice at 10 weeks. Scale bar = 1 mm.

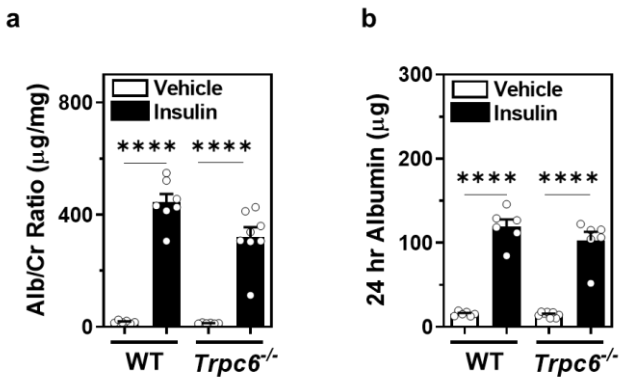


**Supplementary Fig. 4 TRPC6 may not participate in insulin-stimulated proteinuria.**

**a**-**b** Quantitative analysis of 24 h urinary albumin/creatinine (Alb/Cr) ratio (left) (**a**) and albumin excretion (right) (**b**) after administration of insulin (*i.p.;* 5 U/kg) in wild type (WT) and *Trpc6*$^{-/-}$ mice (9-11 weeks old, $n$ = 6, 7, 6, 8 mice each). Data are represented as mean ± SEM and were analyzed using analyzed with two-way ANOVA followed by Tukey's multiple comparisons test (**a** and **b**). ****$p < 0.0001$.

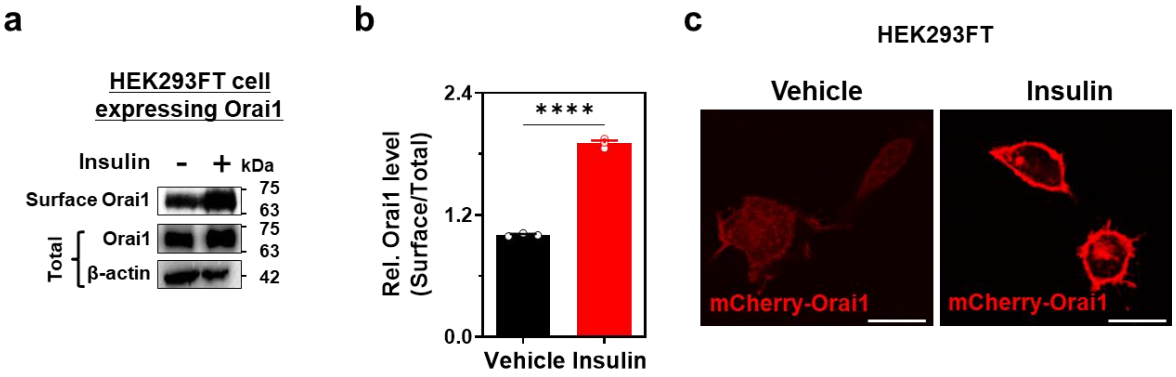


**Supplementary Fig. 5 Insulin increases cell surface abundance of Orai1 in HEK293FT cells**

**a** Biotinylation assay showing the insulin effect (100 nM, 1 h) on the cell-surface abundance of Orai1 in HEK293FT cells transiently expressing mCherry-Flag-tagged Orai1 and YFP-tagged STIM1. **b** Quantification of surface Orai1 by densitometry in three independent experiments of panel (**a**). *n*=3 independent experiments. Data are represented as mean ± SEM and were analyzed using unpaired two-tailed Student's *t*-test. ****$p < 0.0001$. **c** Confocal images showing the effect of insulin treatment on Orai1 localization in HEK293FT cells expressing mCherry-Flag-tagged Orai1. Scale bar = 25 μm.

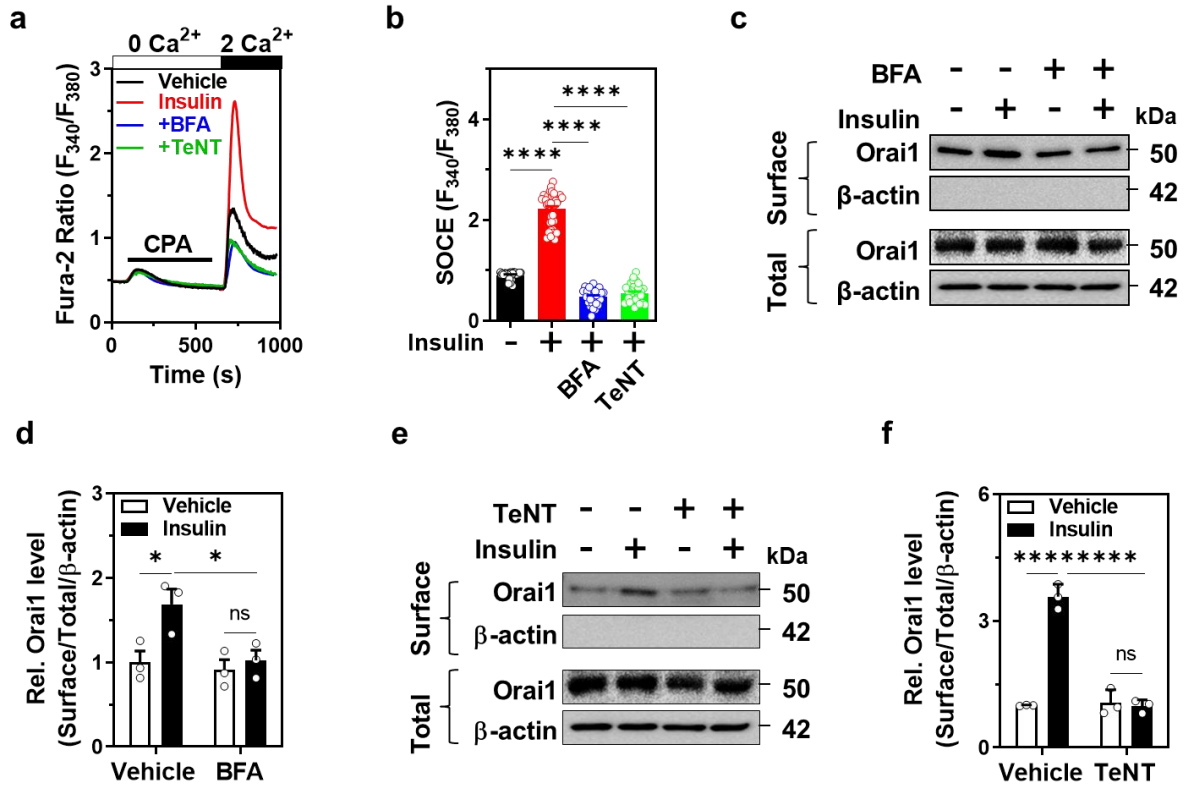


**Supplementary Fig. 6 Insulin increases cell surface abundance of Orai1 by stimulating its exocytosis.**

**a** Representative trace of insulin-stimulated store-operated $Ca^{2+}$ entry **(**SOCE) in addition to brefeldin A (BFA, 10 μM, 8 hr) or tetanus toxin (TeNT, 60 nM, 8 hr). **b** Summary of the SOCE in panel (**a**). *n* = 26, 35, 29, 29 cells per each group. **c**-**f** Biotinylation assay showing the effects of BFA (**c**-**d**) and TeNT (**e**-**f**) treatment on cell surface abundance of Orai1 after insulin stimulation. All the experiments were repeated 3 times independently. Data are represented as mean ± SEM and were analyzed using one-way ANOVA followed by Tukey's multiple comparisons test (**b**, **d**, and **f**). **p* < 0.05, *****p* < 0.0001; ns, not significant.

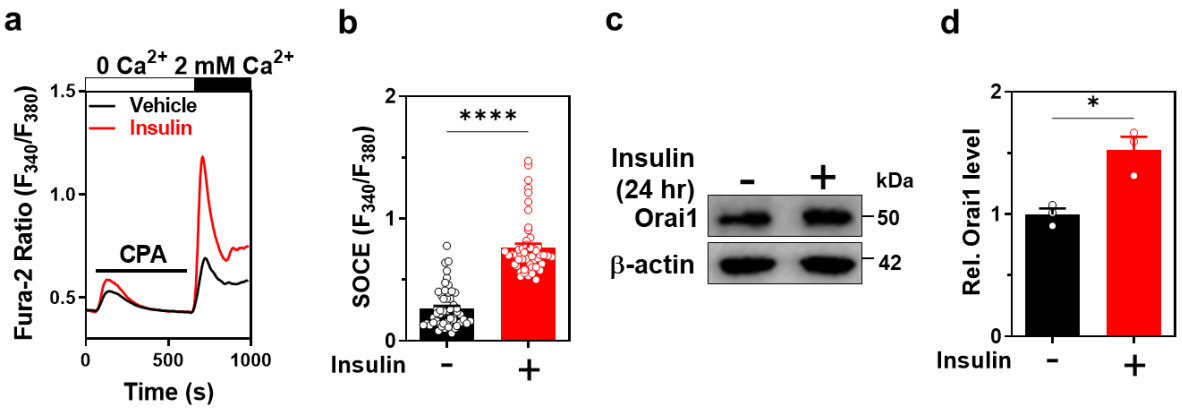


**Supplementary Fig. 7 Effect of long-term incubation of insulin on store-operated $Ca^{2+}$ entry (SOCE) and Orai1 protein expression in podocytes.**

**a** Representative SOCE traces showing the effect of long-term insulin treatment (for 24 h) in cultured mouse podocytes. **b** Summary of the SOCE in panel (**a**). *n* = 53 (Vehicle) and 50 (Insulin) cells. **c** Immunoblotting showing the effect of long-term insulin treatment (for 24 h) on Orai1 expression in podocytes. **d** Summary of the relative (Rel.) Orai1 level in panel (**c**). *n* = 3 independent experiments. Data are represented as mean ± SEM and were analyzed using unpaired two-tailed Student's *t*-test in (**b** and **d**). **p* < 0.01, *****p* < 0.0001.

**a**

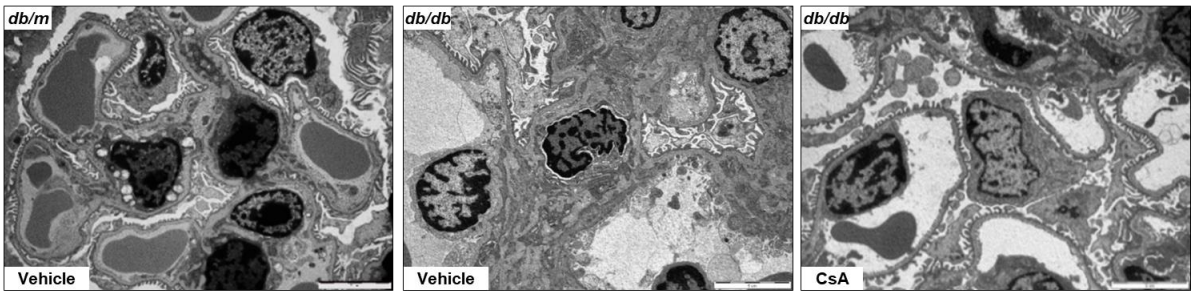


**b**

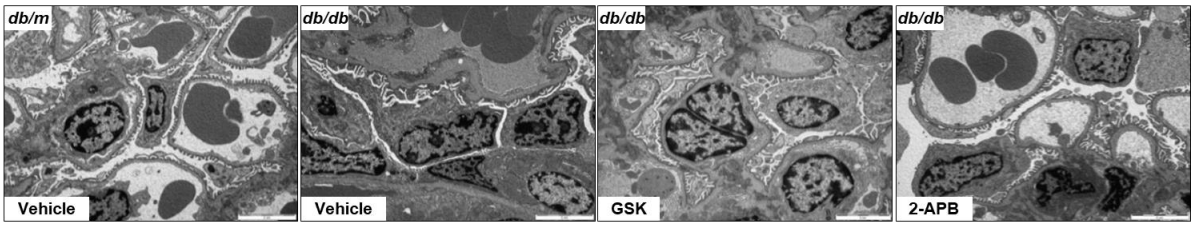


**Supplementary Fig. 8 Representative TAM images in CSA, GSK-7975A, and 2-APB *i.p.* injected *db/db* mice**

**a**-**b** Representative TEM images of kidney tissue in *db/m* and *db/db* mice with administration of CsA (**a**) or GSK or 2-APB (**b**). All images showed similar to the representative images of each group (n = 3 for *db/m*+Vehicle, *db/db*+Vehicle, *db/db*+CsA, *db/db*+GSK, *db/db*+2-APB) and were taken 5 different locations randomly in one mouse. Magnification is 5,000X. Scale bar = 5 μm.

**Supplementary Table 1. List of mouse primer sequences used for PCR.**

| Gene (Accession no.) | Purpose | Primer sequence (5' to 3') | | Size(bp) |
|---|---|---|---|---|
| Mouse 18s (NR_003278.1) | Quantitative real-time PCR | Forward | CGG CGT TAT TCC CAT GAC | 108 |
| | | Reverse | GCC CTT CCG TCA ATT CCT | |
| Mouse Orai1 (NM_175423.3) | Quantitative real-time PCR | Forward | ATG GTA GCG ATG GTG GAA GT | 122 |
| | | Reverse | CTG ATC ATG AGG GCA AAC AG | |
| Mouse Orai2 (NM_178751.3) | Quantitative real-time PCR | Forward | CTG CAT GAG ATC CAC CAC AC | 97 |
| | | Reverse | GGG GAC AGG AGT ATG GGA TT | |
| Mouse Orai3 (NM_198424.3) | Quantitative real-time PCR | Forward | AAC CTC ACA CCA TCC TCT GC | 96 |
| | | Reverse | GCC TGG TCC ATG AGC ACT AT | |
| *Nphs2_Cre* | Genotype | Forward | GCG GTC TGG CAG TAA AAA CTA TC | 100 |
| | | Reverse | GTG AAA CAG CAT TGC TGT CAC TT | |
| *Orai1_flox* | Genotype | Forward | AGG CGG CCT ATA ATT CCA GCT TCA | WT;222<br>*Orai1*$^{fl/-}$;222,378<br>*Orai1*$^{fl/fl}$;378 |
| | | Reverse | AGG TGG ATG TTG CTG AGA GAC CAA | |
| International Positive control | Genotype | Forward | CTA GGC CAC AGA ATT GAA AGA TCT | 324 |
| | | Reverse | GTA GGT GGA AAT TCT AGC ATC ATC C | |